Original article

A study on dosimetric properties of electronic portal imaging device and its use as a quality assurance tool in Volumetric Modulated Arc Therapy

Prabakar Sukumar*, Sriram Padmanaban, Prakash Jeevanandam, S.A. Syam Kumar, Vivekanandan Nagarajan

Medical Physics Department, Cancer Institute (WIA), India

ARTICLE INFO

ABSTRACT

Aim: In this study, the dosimetric properties of the electronic portal imaging device were examined and the quality assurance testing of Volumetric Modulated Arc Therapy was performed.

Background: RapidArc involves the variable dose rate, leaf speed and the gantry rotation. The imager was studied for the effects like dose, dose rate, field size, leaf speed and sag during gantry rotation.

Materials and methods: A Varian RapidArc machine equipped with 120 multileaf collimator and amorphous silicon detector was used for the study. The characteristics that are variable in RapidArc treatment were studied for the portal imager. The accuracy of a dynamic multileaf collimator position at different gantry angles and during gantry rotation was examined using the picket fence test. The control of the dose rate and gantry speed was verified using a test field irradiating seven strips of the same dose with different dose rate and gantry speeds. The control over leaf speed during arc was verified by irradiating four strips of different leaf speeds with the same dose in each strip. To verify the results, the RapidArc test procedure was compared with the X-Omat film and verified for a period of 6 weeks using EPID.

Results: The effect of gantry rotation on leaf accuracy was minimal. The dose in segments showed good agreement with mean deviation of 0.8% for dose rate control and 1.09% for leaf speed control over different gantry speeds.

Conclusion: The results provided a precise control of gantry speed, dose rate and leaf speeds during RapidArc delivery and were consistent over 6 weeks.

© 2011 Greater Poland Cancer Centre, Poland. Published by Elsevier Urban & Partner Sp. z.o.o. All rights reserved.

* Corresponding author at: No. 46 Manimegali Street, East Tambaram, Chennai 600059, Tamil Nadu, India. Tel.: +91 9789882591.
  E-mail address: prabakarsukumar@gmail.com (P. Sukumar).

1.   Background

The potential of direct aperture optimization proposed by Otto as Volumetric Modulated Arc Therapy (VMAT) requires one or more gantry rotations and produces dose distribution equivalent or better than the Intensity Modulated Radiotherapy (IMRT).[1] Varian has introduced volumetric modulation using the RapidArc technique by varying the gantry speed, dose rate and leaf speeds.[2]

To verify the IMRT or RapidArc dose distribution, two-dimensional detectors such as ion chamber arrays, film or diode arrays were used. A film is more frequently used for verification of IMRT dose distributions because of its high resolution. But the dose response of a film is affected by processing conditions. A greater convenience afforded by electronic portal imaging devices has increasingly led to the replacement of a conventional radiographic film by an electronic portal imaging device (EPID) for geometric verification in radiation therapy. The high resolution, high contrast and the large signal to noise ratio and high detective quantum efficiency of EPID made it an alternative to other detectors.

Several authors have extensively studied the dosimetric properties of the aS500 EPID and its applications in IMRT.[3–9] Van Esch et al. evaluated the portal dose prediction model using the algorithm for amorphous silicon (a-Si) detector measurement and tested it for clinical IMRT treatment fields. This prediction model is based on the optimal fluence created in the IMRT optimization. Since RapidArc plan involves a direct MLC optimization, the prediction model cannot be applied for RapidArc plans.

2.   Aim

In this study, the quality assurance of RapidArc was performed using the aS1000 EPID. Since RapidArc involves the variable dose rate, leaf speed and gantry speed, the dosimeter has to be tested for these parameters. Initially, the performance of EPID was verified by investigating the effects of dose, dose rate, field size, leaf speed, and sag due to gantry, jaws, MLC and the imager. The quality assurance tests include accurate positioning of dynamic MLC and a precise control of the dose rate and leaf speed during the gantry rotation. The quality assurance tests were repeated with the film and the results were compared with that of EPID. The tests were performed over a period of 6 weeks to verify the consistency.

3 Materials and methods

3.1 EPID calibration

The aS1000 imaging detector unit (IDU 20 model, Varian Medical Systems, Palo Alto, CA) consists of a 1 mm copper plate, 134 mg/cm^2 gadolinium oxysulphide phosphor screen with the active area of 40 cm × 30 cm a-Si arrays. The spatial resolution of the device is 0.391 mm × 0.391 mm, which is attached to the Linear accelerator Clinac 2100 C/D equipped with millennium multileaf collimator 120 leaves (Varian Medical Systems, Palo Alto, CA) by Exact-arm. The image acquisition software (IAS3) provides several modes for acquisition. Integrated image acquisition is commonly used for dosimetric application. This mode captures a single image consisting of an average of many image frames acquired during radiation delivery. In Image, frame is scanned row by row, with a fixed average frame rate of 9.574 frames/s. For portal dosimetry, the image is acquired in the integrated mode during the radiation delivery.[10]

EPID calibration is designed to remove background noise and provide a spatially uniform response for clinical image. The response of EPID is dependent on the photon energy and the repetition rate of the radiation beam. The detector is calibrated by acquiring flood field and dark field images. The dark field image is acquired by averaging 20 frames without any radiation for offset of the pixel values. The flood field is acquired by the uniform irradiation of the field size larger than the active area of the EPID. Flood field calibration is to determine the difference between the pixel sensitivities. The unit of the electronic portal imager device is calibrated unit (CU). The CU can be calibrated as MU or Gy or cGy. The intrinsic EPID water equivalent made of the copper plate and other materials placed above the phosphor layer is approximately 0.8 cm^3. It is calibrated with ion chamber measurements at the depth of 0.8 cm which is the effective depth (water equivalent depth) of the portal image including the copper. The CU is calibrated in centiGray (1 CU = 1 cGy).

3.2 Dosimetric properties of the electronic portal imaging device

3.2.1 Dose linearity

Dose linearity of the EPID in the integrated mode at 300 MU/min was examined by irradiation with different monitor units ranging from 2 to 500 MU for 10 cm × 10 cm at 100 cm source to detector distance (SDD). The mean pixel value of 3 by 3 matrix at the centre of the field was measured and a graph was plotted against MU. Using the number of frames acquired, the frames/s was calculated for the different dose rate and plotted against MU.

To measure the missing frames, different monitor units were delivered at the constant dose rate and field size at SDD of 100 cm. The missing frame due to the dead time of the
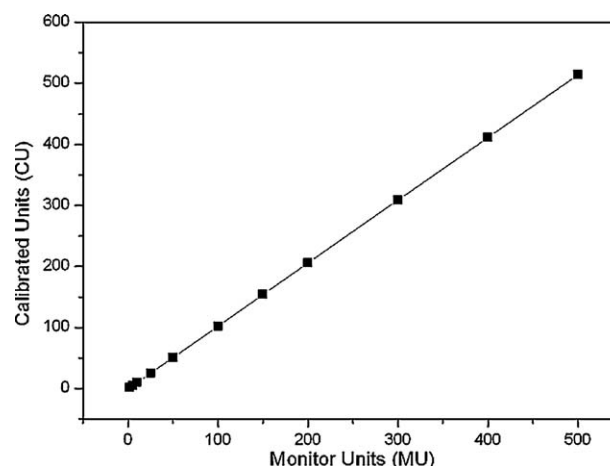

Fig. 1 – Calibrated units to MU linearity.

Table 1 – The missing frame due to dead time in frame acquisition.

| MU	Acquired frames	Time (s)	Time/frame (s)	Calculated frames	Missing frame due to dead time
2	7	0.4	0.05714	7.00035	−0.00035
5	12	1	0.08333	12.00048	−0.00048
10	22	2	0.09091	21.99978	0.00022
25	49	5	0.10204	49.00039	−0.00039
50	98	10	0.10204	98.00079	−0.00079
100	193	20	0.10363	192.9943	0.00569
150	288	30	0.10417	287.9908	0.00922
200	384	40	0.10417	383.9877	0.01229
300	576	60	0.10417	575.9816	0.01843
400	767	80	0.10430	767.0182	−0.01822
500	958	100	0.10438	958.037	−0.037
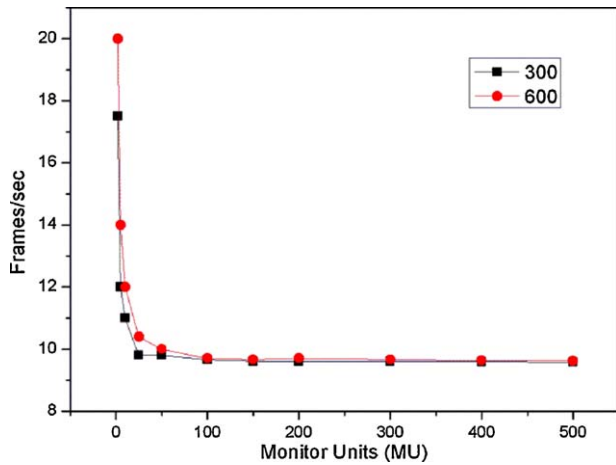
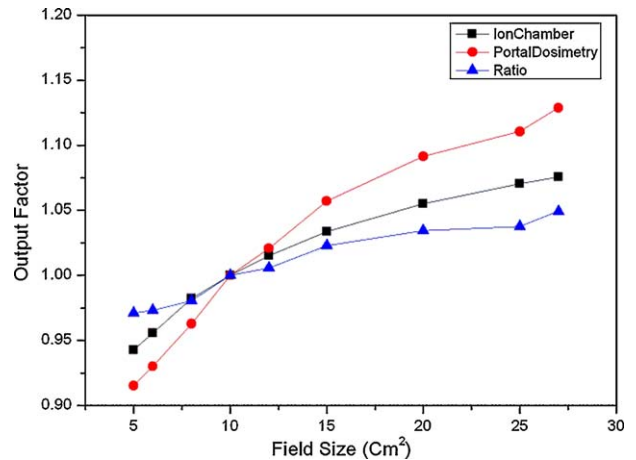Fig. 2 – **Response of frame rate with respect to monitor units.**

Fig. 4 – **Output factor to field size.**

imager was calculated using the number of frames acquired and the time of exposure. The CU/MU ratio should be constant for delivered monitor units. These ratios were compared with ionization chamber measurements.

3.2.2 Dose rate and field size response

The CU for $10\,cm \times 10\,cm$ was measured for different dose rates. The values were measured for five readings for each
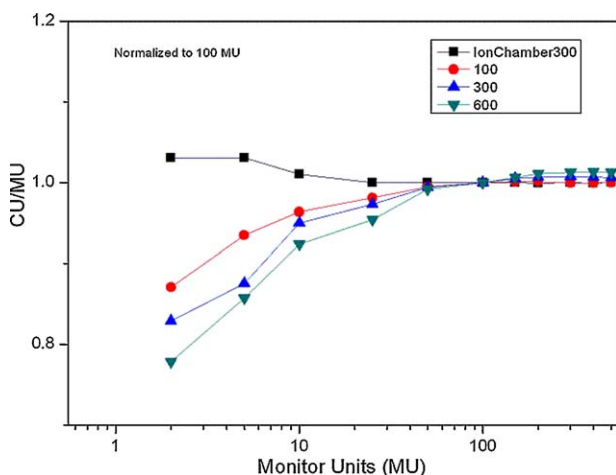
dose rate and an average was calculated. The percentage variation was calculated between the averaged value and averaged value of 300 MU/min.

For different field sizes ranging from $5\,cm \times 5\,cm$ to $27\,cm \times 27\,cm$, 100 MU was delivered at 100 cm SDD. The mean pixel value for 3 by 3 matrix was measured. The output factors were calculated and plotted against field size. The results were compared with those of the ionization chamber measurements.

3.2.3 Effect of leaf speed

To ensure the accuracy of EPID with rapid changes in dose rate during dynamic MLC (DMLC) delivery, a uniform intensity pattern of $10\,cm \times 10\,cm$ using DMLC was delivered. The leaf speed was increased by reducing the monitor units for

Fig. 3 – **Signal ratio vs. monitor units.**

Table 2 – Variation in the CU with dose rate.

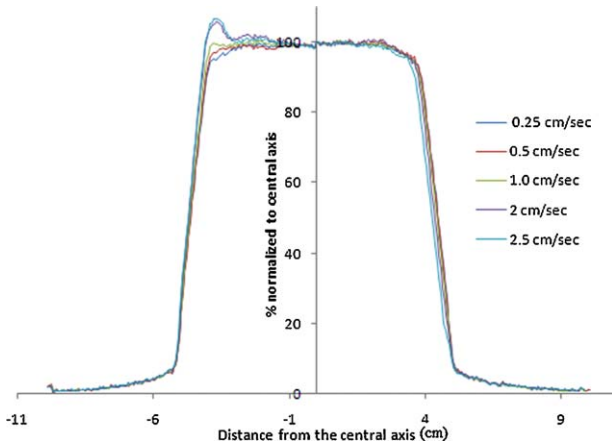| Dose rate (MU/min)	Calibrated units (CU)	Percentage variation (%)
100	101.343	−0.7521
200	102.102	−0.0088
300	102.111	0.0000
400	101.46	−0.6375
500	102.267	0.1528
600	101.522	−0.5768

Fig. 5 – Leaf speed tests with uniform intensity.

constant dose rate of 300 MU/min. Monitor units and corresponding leaf speeds were 20 MU – 2.5 cm/s, 25 MU – 2 cm/s, 50 MU – 1 cm/s, 100 MU – 0.5 cm/s and 200 MU – 0.25 cm/s, respectively. The profile of the DMLC test pattern was compared with the open field profile.

3.2.4 Evaluation of the sag

To evaluate the gravitational sag due to gantry, jaws and EPID, portal images were acquired for a known field size with gantry in static and rotational modes. Portal images were acquired for the field size of 10 cm × 10 cm at SDD of 100 cm at gantry zero degrees. The same number of MUs were delivered in the rotational mode with a constant field size and SDD and an image was acquired. Both images were compared by the Gamma evaluation method using Eclipse planning system software with 3 mm distance to agreement (DTA) and 3% dose difference (DD) criteria.[11,12] To evaluate errors in the MLC during rotation due to sag, the field size was defined by the MLC and the test was repeated.

3.3 Accuracy of the DMLC positioning

To verify the positional accuracy of the DMLC, RapidArc plans of picket fence patterns were compared with the same pattern

acquired with a static gantry. The slits were 1 mm wide at the distance of 1.5 cm. The DMLC positional accuracy for different gantry angles and RapidArc plans was verified by position of the slits in each image. Profiles were taken for each image and the distance between the peaks was measured. The picket fence test with an intentional error of 0.5 mm was performed to access the sensitivity of the imager.

3.4 Control of the dose rate over gantry speed

To verify the control of the dose rate over gantry speed, a RapidArc plan with seven segments of the same dose with varying dose rate and gantry speed (111 MU/min for 90°, 222 MU/min for 45°, 332 MU/min for 30°, 443 MU/min for 22.5°, 554 MU/min for 18°, 600 MU/min for 15° and 600 MU/min for 12.9°) was carried out. To measure the variation in doses, the seven segmented test fields were normalized to the open field delivered with the same MU. 30 MUs were delivered at each segment. The X-omat films had the range of 0–100 cGy and were found to be a linear dose response of up to 80 cGy.[13,14] Since the lower dose is delivered in each segment of the test field, X-omat films were used for the comparison.

The mean pixel values of 3 by 3 matrix in EPID and the mean optical density values in the film were measured at the centre of each segment and normalized to corresponding open fields. The stability of the test results was verified by acquiring images every week and deviations were compared. Using Eq. (1), the pixels values were made independent of the sensitivity and output variation. To calculate the correct pixel values, Eq. (1) was used

$$R_{corr} = \frac{R_{test\ field}(x)}{R_{open\ field}(x)} \times 100 \tag{1}$$

The deviation from the corrected R average readings were calculated using Eq. (2)

$$\text{Percentage Diff}(x) = \left(\left(\frac{R_{corr}(x)}{R_{Corr\ avg}(x)} \right) - 1 \right) \times 100 \tag{2}$$
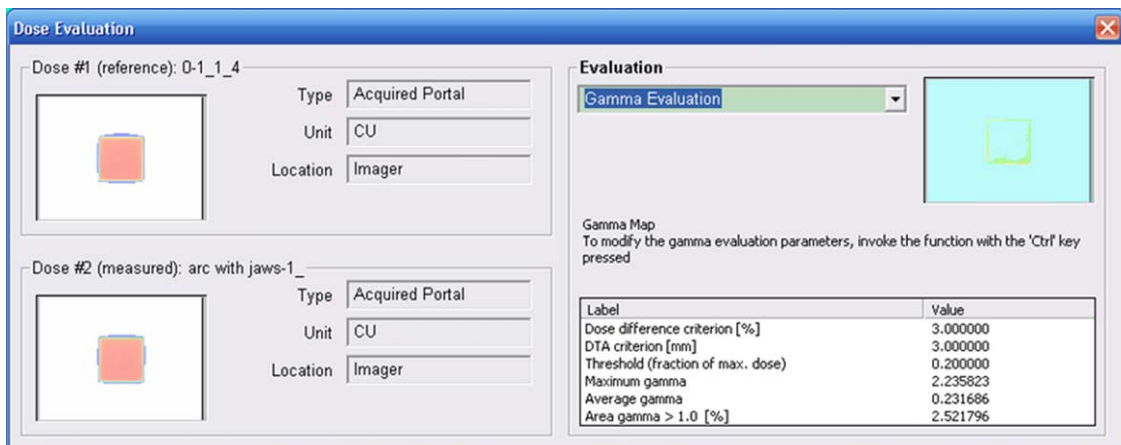

Fig. 6 – Gamma evaluation with field size defined by jaws.

3.5 Control of the leaf speed during RapidArc

To evaluate the ability of the MLC leaf speed control during RapidArc, four uniformly irradiated segmented test patterns were delivered with different combinations of leaf speeds and dose rates. The leaf speed–dose rate combination used in the test patterns were 0.46 cm/s – 138 MU/min, 0.92 cm/s – 277 MU/min, 1.84 cm/s – 554 MU/min – 2.76 cm/s – 554 MU/min, respectively. The width of DMLC fields was 4.5 cm for the last leaf speed segment and 3 cm for the others. The test pattern pixel values were normalized to the open field using Eq. (1) and the deviations were measured using Eq. (2). The test was repeated using the X-Omat films and deviations were calculated. The stability of the test results was verified by acquiring image every week and deviations were compared.

4. Results and discussion

4.1. Dosimetric Properties

4.1.1. Dose linearity

Fig. 1 shows the dose linearity graph. The CU was found to be linear to the dose delivered. The linear fit parameter showed Squared R value equaling one ($R^2 = 1$). Fig. 2 shows the frame acquisition rate vs. MU. The frame acquisition rate increased up to 20 frames/s for dose rate of 600 MU/min and it reached the average frame rate of 9.574 frames/s as monitor units reached the level of 50.

Time per frame is calculated from the known frames and the time of exposure. The missing frame due to dead time is less than a frame as shown in Table 1.

The CU/MU ratios were plotted against monitor units in the logarithmic scale which showed underresponse for lower monitor units. For the ionization chamber measurements, the detector showed overresponse of up to 3%. As the dose rate increased, the detector showed underresponse for lower monitor units (Fig. 3).

4.1.2. Dose rate and field size response

The CU was measured and averaged for each dose rate and the variation was calculated from the standard treatment dose rate of 300 MU/min (Table 2). Even though the CU is calibrated separately for different dose rates, the variation observed was found to be 0.75%. The CUs were measured and the output factor was calculated for different field sizes and plotted. The variation for 5 cm × 5 cm is 2.9% and 5% for 27 cm × 27 cm. This variation was due to the difference in the phantom scatter factor for both ionization chamber and EPID (Fig. 4). Since the scatter has a low energy component, its effect on the EPID's phosphor response is enhanced compared to ionization chamber due to the presence of high atomic number component in the phosphor.
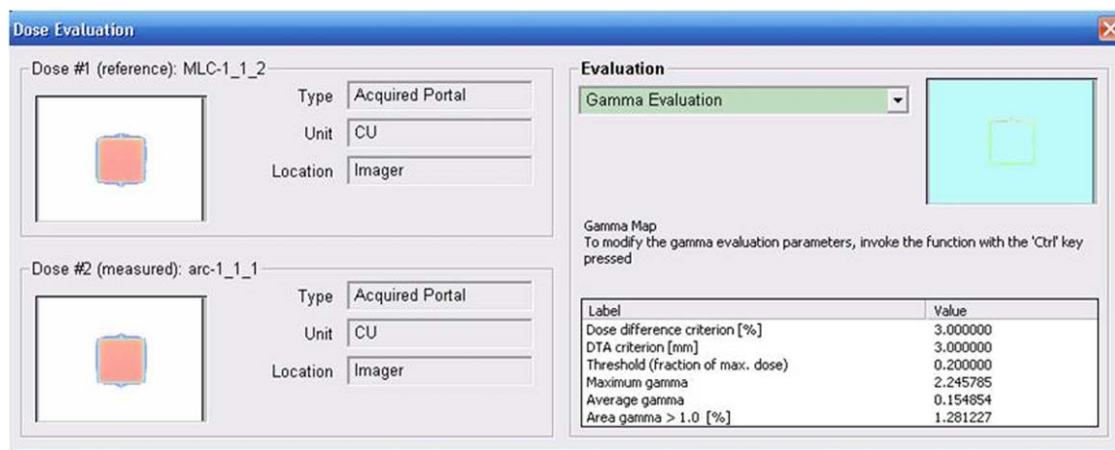

Fig. 7 – Gamma evaluation with field size defined by MLCs.

Table 3 – Percentage deviation in seven segments in RapidArc plan when compared to normalised open field for control of dose rate test.

Positions (cm)	R (DR-GS)	R (op)	$R_{corr}(x)$	diff(x)	S.D.
5	174.866	2896.116	6.037949	1.345172	
−3	179.438	3009.515	5.962356	0.076371	
−1	183.275	3078.608	5.953178	−0.07769	
1	183.753	3095.725	5.935702	−0.37101	0.048227
3	182.969	3060.671	5.978068	0.340095	
5	179.556	3012.325	5.960711	0.048766	
7	169.87	2890.58	5.876675	−1.36176	
		Avg	5.957806		

R (DR-GS) – CU values in the test pattern image; R (op) – CU values in the open field at the same positions of test pattern image.
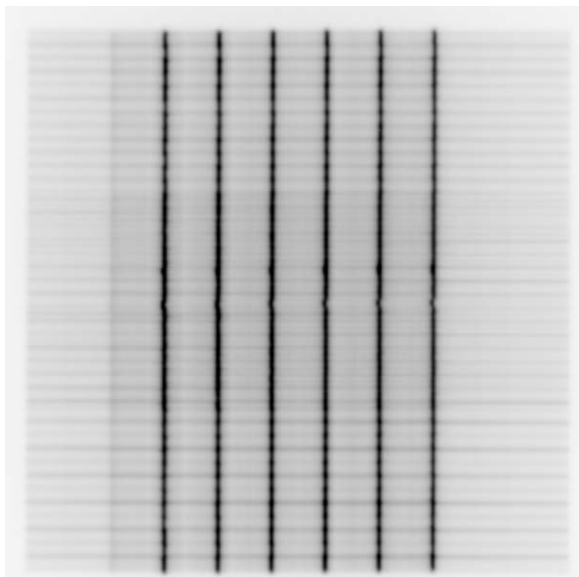
Fig. 8 – Picket fence test with intentional error.

4.1.3. *Effect of leaf speed*

The profiles of different leaf speed patterns were normalized to the central axis and the variations were evaluated (Fig. 5). The variation in profile was pronounced with an increase in leaf speed. For the leaf speed of 2 cm/s and 2.5 cm/s, variation of 4–5% was found in the first segment due to the multi-leaf edge transmission. But the comparison of the images by gamma index method shows the >98% pass criteria in all the leaf speeds.

4.1.4. *Evaluation of the sag*

The area failing the gamma criteria in the field defined by the jaws was due to sag in the gantry and jaws during the rotation. In superior and inferior edges, the area failing was due to gantry and EPID sag, whereas in the left and right edges it was due to the sag in the jaws. The percentage of the area failing the gamma criteria was 2.52% (Fig. 6).

The area failing the gamma criteria in the field defined by the MLC was due to the sag in gantry and MLCs. The area failing gamma criteria was found to be 1.26% in the inferior and superior regions of the field (Fig. 7).

4.2. *Evaluation DMLC positional accuracy*

The image of the delivered picket fence is analysed using the Verisoft software (PTW, Version 3.2). The maximum variations in distances between the peaks were found to be within ±2 mm. The tests showed the accuracy of the DMLC positioning at different gantry angles and during RapidArc plan. The tests with intentional error of 0.5 mm were discerned in the image (Fig. 8). The tests with intentional errors showed that even small errors could to be discerned in the EPID image.

4.3. *Control of dose rate during gantry rotation*

Table 3 shows the percentage deviations in seven segments in RapidArc plan when compared to a normalised open field. The
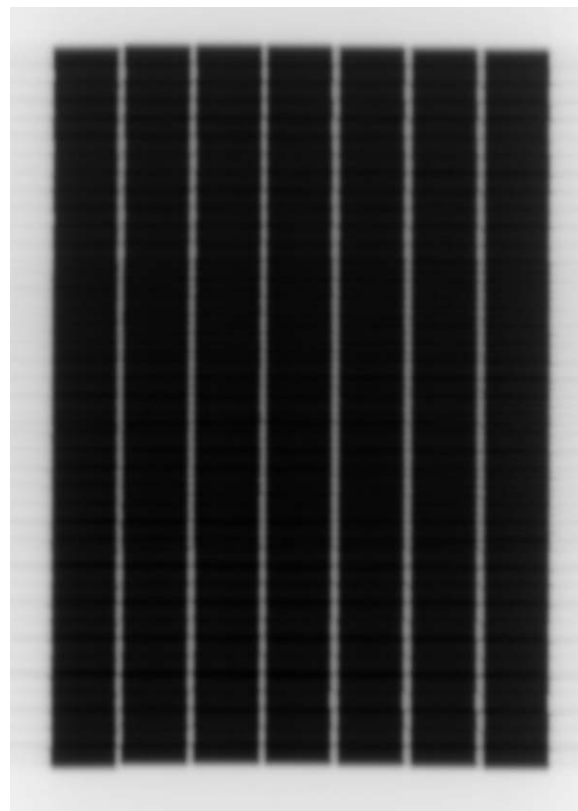

Fig. 9 – Control of dose rate over gantry speed.

variation in all segments was within 2% (Fig. 9). The standard deviation between the segments was found to be 0.8%. For both a film and EPID, the maximum percentage variation was in the first segment (Fig. 10). These results were similar to the leaf speed test carried out with static fields. The stability was good during the period of 6 weeks (Fig. 11).

4.4. *Control of the leaf speed during RapidArc plan*

The pixel values were measured at the centre of the four segments and compared with a normalized open field profile (Fig. 12). Table 4) shows the percentage deviations in four
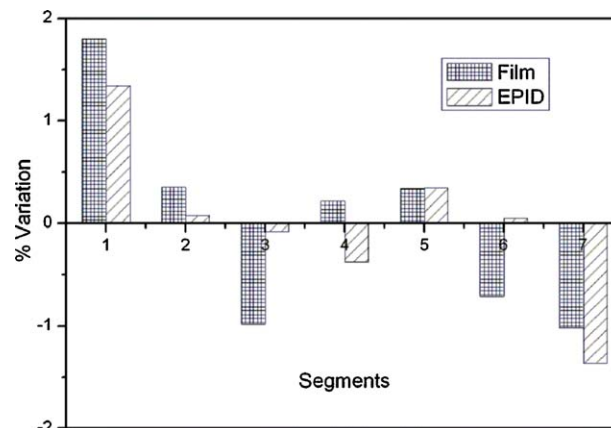

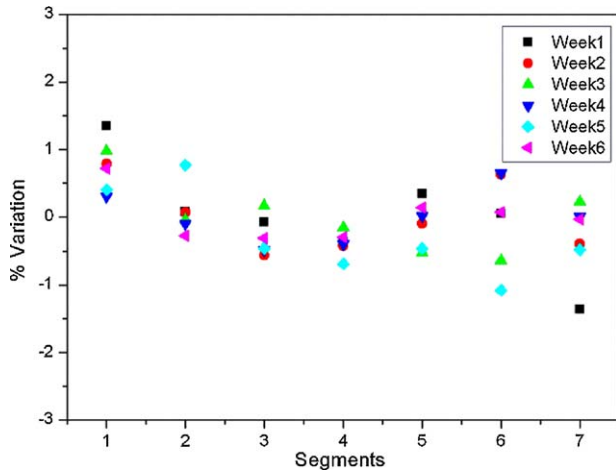**Fig. 10 – Comparison of DS vs. GS film and EPID results.**
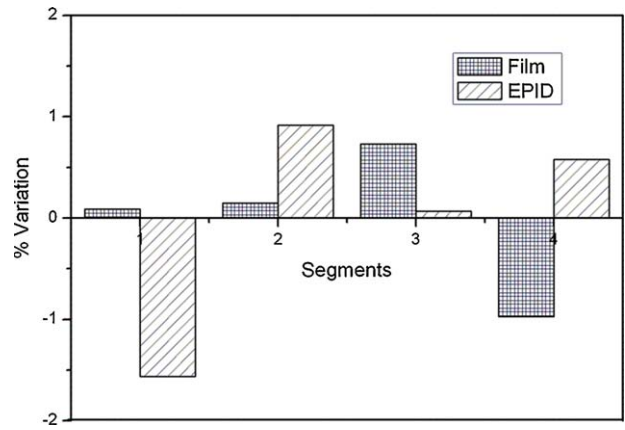
Fig. 11 – DR vs. GS weekly variation of results.

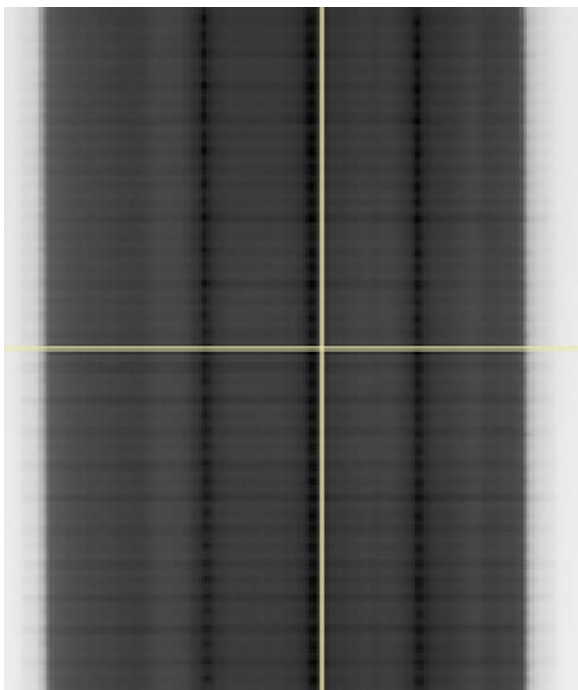**Fig. 13 – Comparison of LS vs. GS film and EPID results.**

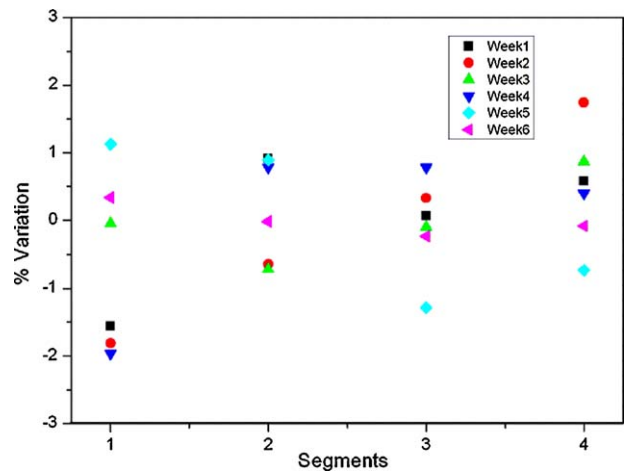**Fig. 12 – Control of leaf speed over gantry speed.**

Fig. 14 – LS vs. GS weekly variation of results.

Table 4 – Percentage deviations in four segments in RapidArc plan when compared to normalised open field for control of leaf speed test.

Positions (cm)	R (LS)	R (op)	$R_{corr}(x)$	diff(x)	S.D.
−4.5	189.519	3404.217	5.567183	−1.56143	
−1.5	202.293	3544.47	5.707285	0.915833	
1.5	200.997	3551.677	5.659214	0.065847	0.062101
4.5	194.477	3418.909	5.688277	0.57973	
		Avg	5.65549		

R (LS) – CU values in the leaf speed test pattern; R (op) – CU values in the open field at same positions.

segments in RapidArc plan when compared to a normalised open field for control of leaf speed test. The standard deviation between four segments was found to be 1.4%. For both the film and EPID, a variation of less than 2% was noted (Fig. 13). The weekly variation was also within 2% (Fig. 14).

5 Conclusion

The dosimetric properties of amorphous silicon EPID were investigated. The EPID has a linear dose response. The maximum variation due to dose rate was 0.8%. Underresponse was detected at the lower monitor units for higher dose rate. The output factor increase for the larger field size was due to backscatter and variation of 5% was observed for the larger field size. The errors due to the leaf speeds during the uniform intensity delivery were also reduced because of the dead time elimination. A maximum variation of 5% was observed at the first segment of the delivery at larger leaf speeds.

This study assessed the MLC positional accuracy, the accuracy of variable dose-rate, and the accuracy of MLC leaf speed during RapidArc using EPID. The weekly variation shows the consistent control over the dose rate and leaf speed during the RapidArc delivery.

REFERENCES

1. Otto K. Volumetric Modulated Arc Therapy: IMRT in a single gantry arc. *Med Phys* 2002;**35**:310–7.
2. Clifton Ling C, Pengpeng Zhang Y, Archambault Y, Bocanek J, Tang G, Losasso T. Commissioning and quality assurance of RapidArc radiotherapy delivery system. *Int J Radiation Oncology Biol Phys* 2008;**72**(2):575–81.
3. Mccurdy BMC, Greer PB. Dosimetric properties of amorphous silicon EPID used in continuous acquisition mode for application to dynamic and arc IMRT. *Med Phys* 2009;**36**(7).
4. Greer PB, Popescu CC. Dosimetric properties of an amorphous silicon electronic portal imaging device for verification of dynamic intensity modulated radiation therapy. *Med Phys* 2004;**31**:285–95.
5. Woźniak B, Ganowicz M, Bekman A, Maniakowski Z. A comparison of the dosimetric properties of the Electronic Portal Imaging Devices (EPIDs) LC250 and aS500. *Rep Pract Oncol Radiother* 2005;**10**(5):249–54.
6. McDermott LN, Wendling M, Van Asselen B, et al. Clinical experience with EPID dosimetry for prostate IMRT pre-treatment dose verification. *Med Phys* 2006;**33**:3921–30.
7. Greer PB. Off-axis dose–response characteristics of an amorphous silicon electronic portal imaging device. *Med Phys* 2007;**34**:3815–24.
8. Pasma KL, Maarten LP, Marco Kroonwijk D. Dosimetric verification of intensity modulated beams produced with dynamic multileaf collimator using an electronic portal imaging device. *Med Phys* 1999;**26**(11):2373–8.
9. Grzadziel A, Smolińska B, Rutkowski R, Ślosarek K. EPID dosimetry – configuration and pre-treatment IMRT verification. *Rep Pract Oncol Radiother* 2007;**12**(6):307–12.
10. Ching J, Ling CC. Using frame averaging of aS500 EPID for IMRT verification. *J Appl Clin Med Phys* 2003;**4**(4):287–99.
11. Low DA, Dempsey JF. Evaluation of Gamma dose distribution comparison method. *Med Phys* 2003;**30**(9):2455–64.
12. Low DA, Harns WB, SasaMutic, Purdy JA. A technique for the quantitative evaluation of dose distribution. *Med Phys* 1998;**25**(5):656–61.
13. Khatib EI, Antolak J, Scrimger J. Evaluation of film and thermoluminescent dosimetry of high energy electron beams in heterogeneous phantoms. *Med Phys* 1992;**29**:2159–68.
14. Dogan N, Leybovich LB, Sethi. A comparative evaluation of Kodak EDR2 and XV2 film for verification of intensity modulated radiation therapy. *Phys Med Biol* 2002;**47**:4121–30.